Repulsive solvent-induced interaction between C_{60} fullerenes in water

Liwei Li, Dmitry Bedrov, and Grant D. Smith
Department of Materials Science & Engineering and Department of Chemical Engineering, University of Utah, 122 S. Central Campus Drive, Room 304, Salt Lake City, Utah 84112, USA
(Received 2 June 2004; published 13 January 2005)

The role of water-fullerene interactions in the behavior of C_{60} in aqueous solution was investigated utilizing realistic Lennard-Jones (LJ) and repulsive Weeks-Chandler-Anderson (WCA) potentials. Strong water-fullerene dispersion interactions in the LJ potential dramatically influence the hydration of the fullerene promoting the formation of a high-density hydration shell of water. In contrast to the WCA potential, the water liquid phase between fullerenes remains stable with decreasing fullerene separation, resulting in a repulsive solvent-induced contribution to the fullerene potential of mean force.

DOI: 10.1103/PhysRevE.71.011502 PACS number(s): 61.20.Ja, 61.20.Ne, 61.48.+c

Various compounds incorporating fullerenes have been recently developed for use in biology and medicine due to their unique structures and properties [1]. For example, C_{60} derivatives have been proposed as HIV protease inhibitors [2]. The size of C_{60} is such that it can be accommodated into the hydrophobic cavity on the protease to block the active sites. The main mechanism of action is supposedly produced only by hydrophobic interactions. Fullerenes have also been decorated to promote interactions with a target molecule, such as a protein on a cell surface [3]. Applications of fullerenes in biomedical imaging [4,5], as antioxidants [6], in biosensors [7,8], and as chemotactic agents [9] are also being explored.

The biological and medical interactions and effects of fullerenes and modified fullerenes are dependent upon the nature of their hydrophobic hydration and hydrophobic interaction in aqueous environments. Understanding of hydrophobic interaction of apolar solutes in water has been elusive due to the multifaceted nature of water [10]. It is known that the hydrophobic effects are related to many factors such as solute size, solute shape, temperature, and strength of the water-solute attractive interaction [11–17]. Much of this understanding is based on the cavity solute model of Chandler [15], which stresses that the hydrophobic effect has significant length scale dependence. The model predicts that, while large hydrophobic surfaces have a disruptive effect on water structure resulting in the tendency of water to dry extended hydrophobic surfaces and hence promote the aggregation of large solutes, the water hydrogen network is predicted to remain intact around small solutes (radii much less than 1 nm). Weak and slowly varying attractive interactions are predicted to have little influence on the water structure and density around the solute and hence can be included by first order perturbation theory with the cavity solute as the reference. Here, we show that the dispersion interaction between water and C_{60} is so strong that the conventional picture of hydrophobic hydration and hydrophobic interaction of apolar solutes drawn from the cavity solute model is not applicable.

Molecular dynamics (MD) simulations were performed at 298 K on a solution of one and two C_{60} fullerenes in 1500 water molecules. An all-atom model was used to represent C_{60}. The carbon-carbon interaction was described by a Lennard-Jones (LJ) potential

$$U_{\mathrm{LJ}}(r) = 4\varepsilon\left[\left(\frac{\sigma}{r}\right)^{12} - \left(\frac{\sigma}{r}\right)^{6}\right] \tag{1}$$

with $\sigma_{CC}=3.47$ Å and $\varepsilon_{CC}=0.275$ kJ mol^{-1} as utilized extensively in previous simulations of C_{60} [18]. The transferable intermolecular four-point potential (TIP4P) model was employed to describe water-water interactions [19]. For the interactions between C_{60} and water, a realistic LJ potential ($\sigma_{CO}=3.19$ Å, $\varepsilon_{CO}=0.392$ kJ mol^{-1}) was utilized. This potential was systematically developed by Werder *et al.* to accurately recover the macroscopic contact angle of a water droplet on a graphite sheet [20]. Additionally, simulations utilizing the Weeks-Chandler-Anderson (WCA) [21] form of this water-fullerene potential,

$$U_{\mathrm{WCA}}(r) = \begin{cases} U_{\mathrm{LJ}}(r) + \varepsilon, & r \leqslant r_{\min} = 2^{1/6}\sigma, \\ 0, & r > r_{\min}, \end{cases} \tag{2}$$

were also performed. The WCA potential has the same shape as the LJ potential up to the minimum in the LJ potential, but does not include the attractive dispersion tail of the LJ interaction: the WCA potential is purely repulsive. MD simulations were carried out using the simulation package LUCRETIUS described elsewhere [22]. The SHAKE algorithm [23] was employed to constrain the bond lengths. Additional bonds were added to keep the fullerenes rigid. The particle mesh Ewald algorithm [24] was used to treat the long-range water-water Coulomb interactions, while LJ interactions were truncated at 10 Å. All simulations were performed in periodic cubic (one fullerene) or orthorhombic (two fullerenes) cells. After equilibration of the solutions at atmospheric pressure using an *NPT* ensemble, sampling was carried out in the *NVT* ensemble with an approximate running length of 10 ns (single fullerene) or 15 ns per umbrella window (two fullerenes, see below) employing a multiple time step reversible reference system propagator algorithm [25,26].

Figure 1 shows the density of interfacial water relative to that of bulk water as a function of interface thickness r (measured from the surface of the fullerene) for a single fullerene with LJ and WCA water-fullerene interactions, determined from the relationship

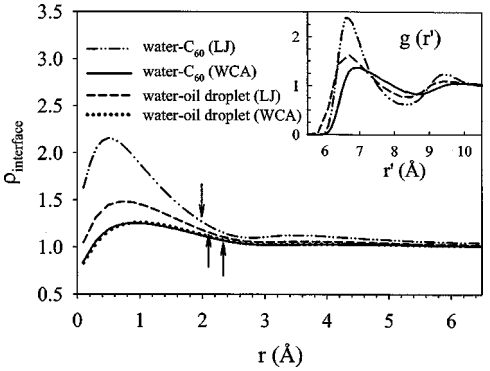

FIG. 1. The relative density of interfacial water as a function of interface thickness (relative to the surface of a C_{60} fullerene) for various water-C_{60} potentials. The arrow shows the first hydration shell. The inset shows the water-C_{60} pair distribution function as a function of the distance between the fullerene center of mass and the water oxygen atom.

$$\rho_{\text{interface}}(r) = \frac{\int_{r'_{1/2\max}}^{r'_{1/2\max}+r} g_{\text{water-C}_{60}}(r')r'^2 dr'}{\int_{r'_{1/2\max}}^{r'_{1/2\max}+r} r'^2 dr'} \tag{3}$$

where $g_{\text{water-C}_{60}}(r')$ is the water-fullerene radial distribution function (RDF) as a function of distance r' between the fullerene center of mass and the water oxygen atom, shown in the inset of Fig. 1. The fullerene surface is considered to correspond to the value of r' where $g_{\text{water-C}_{60}}(r')$ has reached half of its maximum value. By comparing the water-C_{60} RDFs obtained from simulations using the LJ and WCA water-C_{60} potentials and the corresponding interfacial densities, it is clear that the attractive tail of the LJ water-C_{60} potential, due to dispersion interactions between the carbon atoms of the fullerene and water, significantly perturbs the density of water hydrating the fullerene. Indeed, while the WCA water-C_{60} interaction leads to little increase in density of interfacial water compared to bulk water, the LJ potential leads to a dramatic excess of interfacial water in the first hydration shell.

The potential of mean force (PMF) $[\Delta W(r)]$ as a function of distance between the surfaces of two fullerenes in a dilute solution is given by

$$\Delta W(r) = -k_B T \ln g_{\text{C}_{60}\text{-C}_{60}}(r+d) \tag{4}$$

where $g_{\text{C}_{60}\text{-C}_{60}}(r+d)$ is the RDF obtained from simulations of two fullerenes in water, d is the diameter of a fullerene, and $r+d$ is the center-of-mass separation of the two fullerenes. We determined the fullerene diameter to be 9.48 Å based upon the PMF of two C_{60} fullerenes in vacuum at 298 K where d is the center-of-mass separation at which the PMF of two fullerenes in vacuum is equal to its large-separation value (defined to be zero). In our simulations, an umbrella sampling technique [27] combined with a self-consistent multiple histogram method [28,29] was used to sample $g_{\text{C}_{60}\text{-C}_{60}}(r+d)$ accurately and obtain $\Delta W(r)$. A harmonic

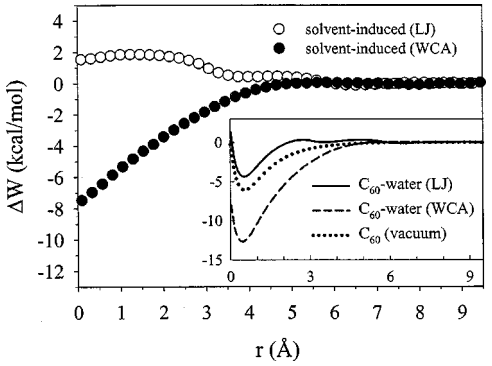

FIG. 2. The solvent-induced contribution to the potential of mean force between two C_{60} fullerenes in water for the LJ and WCA water-C_{60} potentials. The inset shows the total potential of mean force between C_{60} fullerenes in water and vacuum.

spring connecting the centers of mass of the two fullerenes was utilized with nine windows to cover C_{60}-C_{60} surface separations from 0 to 9 Å. The PMF between two C_{60} fullerenes in water for both the LJ and WCA water-fullerene potentials as well as the PMF between two fullerenes in vacuum are shown in the inset of Fig. 2. The PMF was arbitrarily set to zero when the two fullerenes were well separated. Each PMF curve is characterized by a striking minimum at a distance corresponding to C_{60}-C_{60} contact, indicating a strong tendency for aggregation of C_{60} at 298 K whether in water solvent or in vacuum.

Subtracting the PMF of the fullerenes in vacuum from that obtained in water solvent yields the solvent-induced contribution to the PMF:

$$\Delta W_{\text{induced}}(r) = \Delta W(r) - \Delta W_{\text{vacuum}}(r) \tag{5}$$

as shown in Fig. 2. It is clear that the pronounced minimum in the total PMF (inset to Fig. 2) is due to the direct C_{60}-C_{60} interaction. Once this direct interaction is subtracted, it becomes apparent that water actually promotes the *dispersion* of C_{60} fullerenes, indicated by a positive (repulsive) value of $\Delta W_{\text{induced}}(r)$ for all r. However, when the strong dispersion interactions between the fullerenes and water are neglected, there is a strong hydrophobic interaction between the fullerenes as evidenced by the increasingly attractive (negative) $\Delta W_{\text{induced}}(r)$ found for the WCA water-C_{60} potential with decreasing separation between fullerenes.

In order to better understand the qualitative difference in $\Delta W_{\text{induced}}(r)$ obtained using the realistic LJ and repulsive WCA water-C_{60} potentials, we have further analyzed the structure of water hydrating the C_{60} fullerene. In Fig. 3(a) we show the number of water-water hydrogen bonds per oxygen atom, considered to form when the O···O distance is less than 3.4 Å and the O—H···O angle is less than 30°, as a function of distance from the C_{60} surface obtained from simulations with a single fullerene in water. Figure 3(a) reveals that while there is a reduction in the extent of water-water hydrogen bonding in the first hydration shell (the arrow shows the boundary of the shell) of the fullerene for the LJ water-C_{60} potential compared to bulk water (N_h=1.75), this reduction is much less severe than for the WCA water-

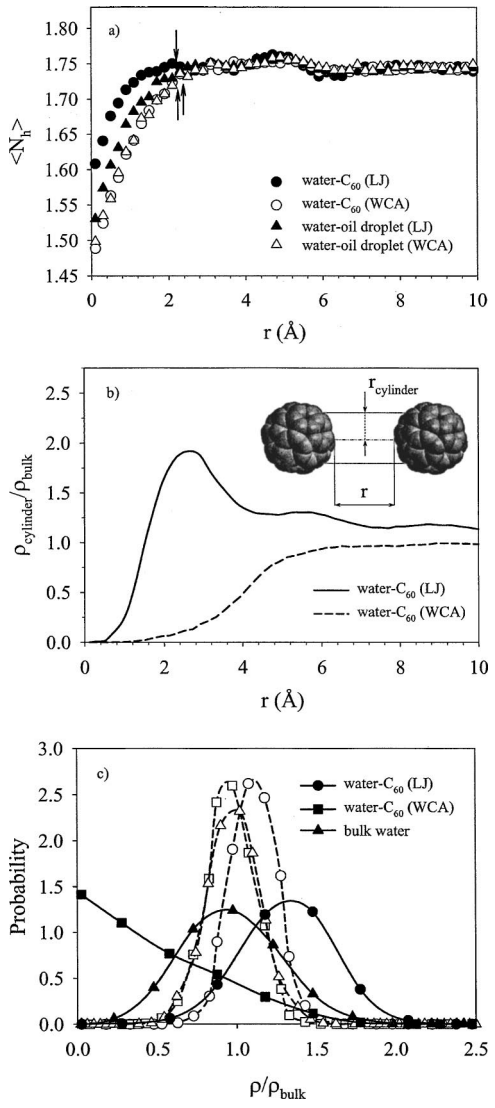

FIG. 3. Comparison of the structure of interfacial water for the LJ and WCA water-C_{60} potentials. (a) Number of water-water hydrogen bonds per oxygen as a function of distance from the fullerene surface for various potentials; the arrow indicates the first hydration shell. (b) Relative density of water in a cylinder of radius 3.5Å between two C_{60} fullerenes as a function of separation between fullerene surfaces. (c) Distribution of densities in the cylinder between two C_{60} fullerenes for separations 4.0 (filled symbols) and 10.0Å (open symbols) for the LJ and WCA water-C_{60} interactions as well as the density distribution in the equivalent volume in bulk water.

C_{60} potential. The high density of water in the first hydration shell (Fig. 1) for the LJ water-C_{60} potential allows water to maintain a high degree of hydrogen bonding despite the presence of the apolar C_{60} surface. A total of 1.7 water-water hydrogen bonds are lost upon adding the C_{60} fullerene to the water solution when the realistic LJ-water potential is utilized, compared to 5.5 with the WCA water-C_{60} interaction.

In Fig. 3(b) we show the relative density (compared to bulk water) of water in a cylinder of radius 3.5 Å centered on the line of the closest approach of two C_{60} fullerenes (as illustrated on the inset) as a function of separation between C_{60} surfaces. Figure 3(b) reveals that interfacial water between two fullerenes remains stable down to separations of about 3 Å, corresponding to a single water layer between the fullerenes, for the LJ water-C_{60} interaction. The stable "layering" of water around the fullerenes with a period of 3 Å revealed in Figs. 3(b) and 1 accounts for the structure in $\Delta W_{\text{induced}}(r)$ seen in Fig. 2 for the LJ water-C_{60} potential. In contrast, the density of water between fullerenes decreases rapidly for the WCA water-C_{60} potential for separations less than 5 Å, corresponding to the separation where $\Delta W_{\text{induced}}(r)$ becomes attractive (Fig. 2). The relative stability of water between the fullerenes for the two potentials can be compared by examining fluctuations in density in the cylinder for representative separations, as shown in Fig. 3(c). This figure illustrates that at large C_{60} separation (10 Å) the density fluctuations are almost Gaussian around the bulk water density. A slight shift of the distribution to the larger than bulk water densities for the LJ water-C_{60} interaction is consistent with the increased water density at the fullerene surfaces observed in Fig. 1. When the separation is reduced to 4 Å, the distributions for the LJ water-C_{60} interaction and for bulk water become broader but still roughly Gaussian. However, the distribution for the WCA water-C_{60} interaction is no longer Gaussian and the most probable density corresponds to vaporlike values. The latter clearly illustrates the destabilization of the liquid water phase between two fullerenes for the WCA water-C_{60} interaction.

Figures 1–3 reveal that the strong dispersion interactions between water and C_{60} dramatically influence the hydration of C_{60}, the hydrophobic interaction between C_{60} fullerenes, and the stability of water between fullerenes at close separations. Indeed, despite the fact that the fullerene does not form strong specific bonds (hydrogen bonds) with water, or have strong electrostatic (polar) interactions with water, the dispersion interactions between water and C_{60} are sufficiently strong. This strong favorable interaction between water and C_{60} is consistent with apparently observed wettability of graphite sheets [30–33]. This also implies that traditional concepts of hydrophobic hydration and hydrophobic interactions might not be applicable to solutions of C_{60} in water. While C_{60} is clearly not soluble in water, as evidenced by $\Delta W(r)$ shown in Fig. 2 (inset), the aggregation of C_{60} is driven by very strong C_{60}-C_{60} attraction and not by hydrophobic interaction. The strong C_{60}-C_{60} attraction is a consequence of the high atomic density on the surface of the C_{60} which leads to strong water-C_{60} and even stronger C_{60}-C_{60} dispersion interactions.

In order to compare the behavior of C_{60} in water with that of a more conventional apolar species, we determined the potential for interaction of water with an "oil" droplet of the same diameter as a C_{60} fullerene in the following way. A simulation of a bulk melt of linear alkane $C_{10}H_{22}$ molecules was conducted using an all-atom potential [34] at 298 K and atmospheric pressure. For each trajectory snapshot (saved every picosecond) a sphere of radius 4.25 Å was placed at a random position in the simulation cell. All atoms inside the sphere were considered to constitute an "oil" droplet. A test water molecule was then inserted in 1000 random locations in the cell and its interaction with the oil droplet atoms was calculated utilizing LJ potential of an existing water-ether

force field [35] and was averaged as a function of separation from the center of the oil droplet. The water-C_{60} LJ parameters were then adjusted ($\sigma_{CO}=3.24$ Å, $\varepsilon_{CO}=0.096$ kJ mol^{-1}) so that the averaged (over all possible orientations) interaction as a function of water-C_{60} center-of-mass separation was equivalent to that for the water-oil droplet determined as described above. This potential yields a minimum (most favorable) water-oil droplet energy of -0.80 kJ mol^{-1}, compared with -2.93 kJ mol^{-1} for the water-C_{60} potential. This difference in attraction reflects the high density of surface atoms in the fullerene. Figure 1 shows the density of interfacial water obtained for the LJ water-oil droplet and corresponding WCA potential. The density of interfacial water for the WCA water-oil droplet potential is essentially identical to that obtained for the WCA water-C_{60} potential. While some increase in the density of interfacial water can be seen for the weakly attractive LJ water-oil droplet potential compared to the WCA potentials, the increase is minor compared to that observed for the LJ water-C_{60} potential. Similarly, Fig. 3(a) reveals that the extent of water hydrogen bonding near the weakly attractive oil droplet more closely resembles that found for WCA water-C_{60} and WCA water-oil droplet interactions than the strongly attractive LJ water-fullerene interactions. A total of 3.9 water-water hydrogen bonds are lost upon addition of the weakly attractive oil droplet compared to 5.5 for the WCA oil droplet and 1.7 for the C_{60} fullerene with LJ water-fullerene interactions.

In summary, our simulations reveal that strong dispersion interactions between C_{60} fullerenes are responsible for their aggregation in water. Strong dispersion interactions between C_{60} and water result in a positive (repulsive) solvent-induced contribution to the potential of mean force between C_{60} fullerenes. A consequence of these strong interactions is that traditional concepts of hydrophobic hydration and hydrophobic interactions based on the cavity model, which are applicable in the presence of weak water-solute interactions, are not applicable to water-C_{60} solutions.

The authors would like to acknowledge NSF support through Grants No. DMR0076306 and No. ITR-CHE0312226. We also would like to thank R. L. Jaffe (NASA-Ames) for helpful discussions.

[1] W. H. Noon, Y. Kong, and J. Ma, Proc. Natl. Acad. Sci. U.S.A. **99**, 6466 (2002).
[2] G. L. Marcorin, T. D. Ros, S. Castellano, G. Stefancich, I. Bonin, S. Miertus, and M. Prato, Org. Lett. **2**, 3955 (2000).
[3] J. Gorman, Sci. News (Washington, D. C.) **162**, 26 (2002).
[4] D. W. Cagle, S. J. Kennel, S. Mirzadeh, J. M. Alford, and L. J. Wilson, Proc. Natl. Acad. Sci. U.S.A. **96**, 5182 (1999).
[5] T. Wharton, J. M. Alford, L. O. Husebo, and L. J. Wilson, in *Recent Advances in the Chemistry and Physics of Fullerenes and Related Materials* (Electrochemical Society, Pennington, NJ, 2000), Vol. 9, p. 258.
[6] N. Tsao, T.-Y. Luh, C.-K. Chou, T.-Y. Chang, J.-J. Wu, C.-C. Liu, and H.-Y. Lei, J. Antimicrob. Chemother. **49**, 641 (2002).
[7] H. T. Tien and A. L. Ottova, Electrochim. Acta **43**, 3587 (1998).
[8] I. Szymanska, H. Radecka, J. Radecki, and D. Kikut-Ligaj, Biosens. Bioelectron., **16**, 911 (2001).
[9] C. Toniolo, A. Bianco, M. Maggini, G. Scorrano, M. Prato, M. Marastoni, R. Tomatis, S. Spisani, G. Palu, and E. D. Blair, J. Med. Chem. **37**, 4558 (1994).
[10] D. Chandler, Nature (London) **417**, 491 (2002).
[11] L. R. Pratt and D. Chandler, J. Chem. Phys. **73**, 3434 (1980).
[12] D. M. Huang and D. Chandler, Proc. Natl. Acad. Sci. U.S.A. **97**, 8324 (2000).
[13] D. M. Huang and D. Chandler, J. Phys. Chem. B **106**, 2047 (2002).
[14] K. Lum, D. Chandler, and J. D. Weeks, J. Phys. Chem. B **103**, 4570 (1999).
[15] D. Chandler (unpublished).
[16] H. S. Ashbaugh and M. E. Paulaitis, J. Am. Chem. Soc. **123**, 10721 (2001).
[17] J. Hernández-Cobos, A. D. Mackie, and L. F. Vega, J. Chem. Phys. **114**, 7527 (2001).
[18] L. A. Girifalco, J. Phys. Chem. **96**, 858 (1992).
[19] W. L. Jorgensen, J. Chandrasekhar, J. D. Madura, R. W. Impey, and M. Klei, J. Chem. Phys. **79**, 926 (1983).
[20] T. Werder, J. H. Walther, R. L. Jaffe, T. Halicioglu, and P. Koumoutsakos, J. Phys. Chem. B **107**, 1345 (2003).
[21] J. D. Weeks, D. Chandler, and H. C. Andersen, J. Chem. Phys. **54**, 5237 (1971).
[22] http://www.che.utah.edu/~gdsmith/mdcode/main.html
[23] J. P. Ryckaert, G. Ciccotti, and H. J. C. Berendsen, J. Comput. Phys. **23**, 327 (1977).
[24] U. Essmann, L. Perera, M. L. Berkowitz, T. Darden, H. Lee, and L. G. Pedersen, J. Chem. Phys. **103**, 8577 (1995).
[25] M. Tuckerman, B. J. Berne, and G. J. Martyna, J. Chem. Phys. **97**, 1990 (1992).
[26] M. Tuckerman, B. J. Berne, and G. J. Martyna, J. Chem. Phys. **94**, 6811 (1991).
[27] G. M. Torrie and J. P. Valleau, J. Comput. Phys. **23**, 187 (1977).
[28] A. M. Ferrenberg and R. H. Swendsen, Phys. Rev. Lett. **63**, 1195 (1989).
[29] D. Bedrov, G. D. Smith, and J. S. Smith, J. Chem. Phys. **119**, 10438 (2003).
[30] F. M. Fowkes and W. D. Harkins, J. Am. Chem. Soc. **62**, 3377 (1940).
[31] L. Morcos, J. Chem. Phys. **57**, 1801 (1972).
[32] M. E. Tadros, P. Hu, and A. W. Adamson, J. Colloid Interface Sci. **49**, 184 (1974).
[33] M. E. Schrader, J. Phys. Chem. **84**, 2774 (1980).
[34] G. D. Smith and D. Y. Yoon, J. Chem. Phys. **100**, 649 (1994).
[35] G. D. Smith, O. Borodin, and D. Bedrov, J. Comput. Chem. **23**, 1480 (2002).